Atomic insights into the mechanisms of Al^{3+} or Cr^{3+} affecting ferrihydrite nucleation

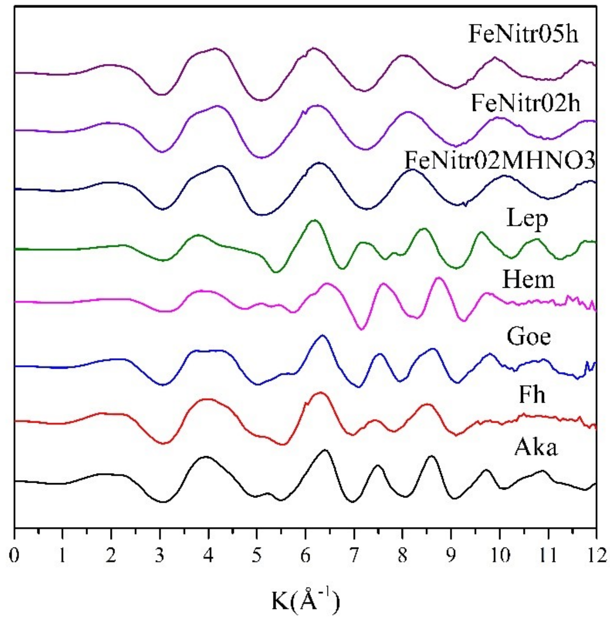

S.I. 1 EXAFS spectra of Fe hydroxide minerals (Fh, Goe, Hem, Aka, Lep) and aqueous Fe species (FeNitr02MHNO3, FeNitr02h and FeNitr05h) from (Zhu et al., 2016).

S.I. 2 The molar fractions of μ-oxo dimer, $Fe(H_2O)_6^{3+}$, $Fe(OH)(H_2O)_6^{2+}$ and $Fe(OH)_3(H_2O)_3$ in FeNitr02MHNO3, FeNitr02h and FeNitr05h (Zhu et al., 2016).

Standards	μ-oxo dimer	$Fe(H_2O)_6^{3+}$	$Fe(OH)(H_2O)_6^{2+}$	$Fe(OH)_3(H_2O)_3$
FeNitr05h	0.470	0.477	0.053	1.26×10^{-10}
FeNitr02h	0.271	0.689	0.040	2.63×10^{-11}
FeNitr02MHNO3	0.128	0.843	0.028	5.72×10^{-12}

S.I. 3 Time-resolved UV-Vis spectra of the immediate products during the ferrihydrite formation in three systems.

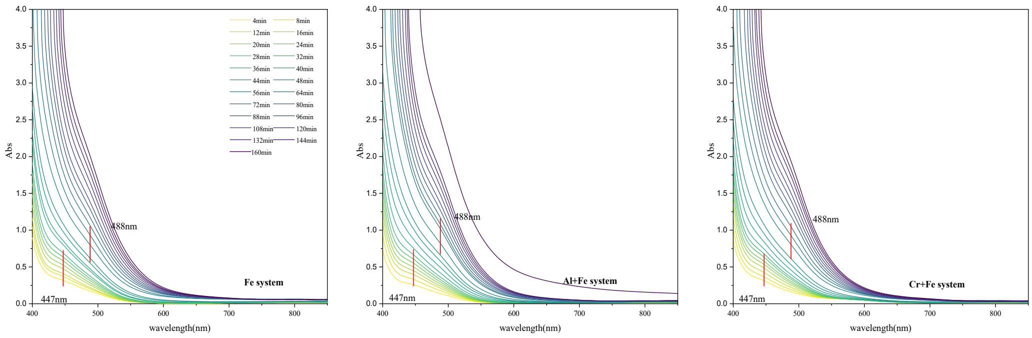

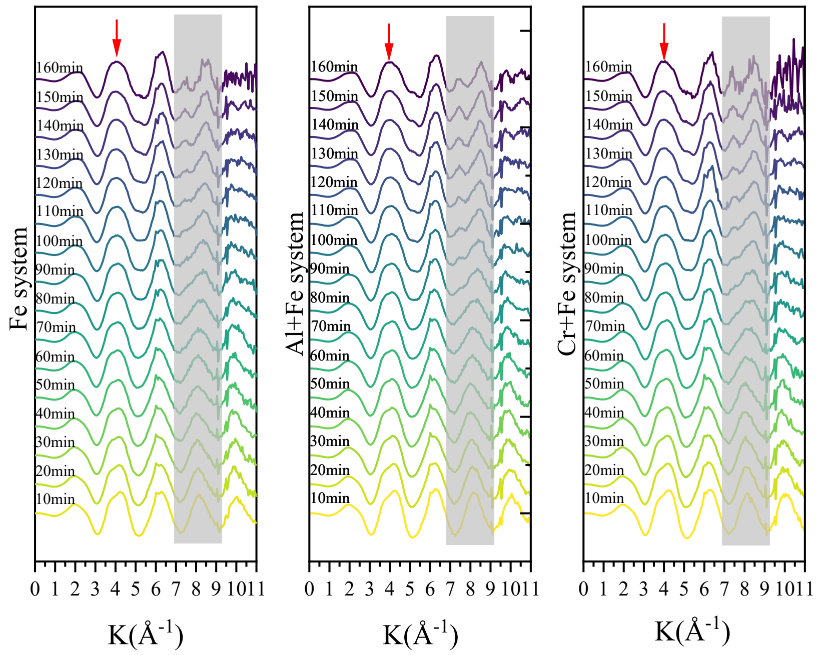

S.I. 4 Time-resolved Fe K-edge EXAFS spectra of reaction intermediates in the three systems.

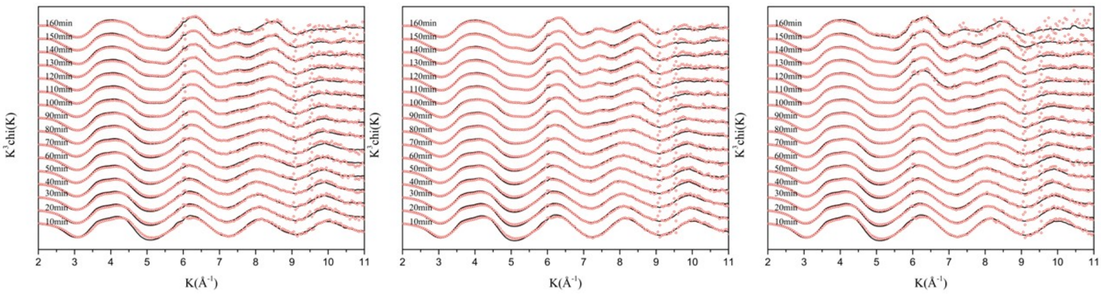

S.I. 5 Linear combination fitting of Fe K-edge EXAFS spectra of the reaction intermediates in the three systems (red circles is experimental data; black line is fitting data. Left: Fe system, middle: Al+Fe system, right: Cr+Fe system)

S.I. 6 Evolution of the proportions of various Fe species with time during the ferrihydrite formation in the Fe system.

Time (min)	ferrihydrite	error	μ-oxo dimer	error	$Fe(H_2O)_6^{3+}$	error	$Fe(OH)(H_2O)_6^{2+}$	error
10	0.00%	/	37.90%	4.17%	57.48%	8.87%	4.57%	0.56%
20	8.40%	13.30%	40.34%	5.05%	46.59%	10.95%	4.67%	0.70%
30	11.50%	2.40%	43.68%	1.13%	40.09%	1.14%	4.84%	0.13%
40	12.10%	5.70%	44.65%	4.41%	38.34%	9.39%	4.93%	0.60%
50	19.20%	4.30%	42.89%	5.85%	33.18%	11.37%	4.65%	0.78%
60	28.00%	3.50%	34.20%	3.28%	33.94%	5.89%	3.87%	0.43%
70	33.70%	2.60%	31.82%	1.22%	30.59%	1.24%	3.90%	0.14%
80	39.20%	2.50%	28.84%	1.18%	28.73%	1.19%	3.22%	0.13%
90	47.60%	2.10%	24.06%	0.99%	25.61%	1.00%	2.74%	0.11%
100	52.80%	4.10%	19.84%	1.87%	25.01%	3.68%	2.35%	0.24%
110	58.30%	9.60%	16.02%	5.05%	23.69%	7.82%	1.99%	0.63%
120	62.70%	9.70%	16.33%	5.13%	19.08%	7.93%	1.88%	0.64%
130	68.70%	9.40%	12.85%	9.18%	16.93%	23.58%	1.51%	1.33%
140	80.20%	4.70%	8.03%	2.14%	10.84%	4.17%	0.91%	0.28%
150	85.10%	10.90%	6.75%	5.77%	7.39%	8.91%	0.75%	0.72%
160	91.30%	2.80%	1.64%	1.32%	6.90%	1.34%	0.23%	0.15%

S.I. 7 Percentage of different Fe species with time in the Al+Fe system.

Time (min)	ferrihydrite	error	μ-oxo dimer	error	$Fe(H_2O)_6^{3+}$	error	$Fe(OH)(H_2O)_6^{2+}$	error
10	0.00%	/	29.63%	2.03%	66.29%	4.49%	4.02%	0.28%
20	0.00%	/	36.56%	4.84%	58.83%	17.36%	4.61%	0.79%
30	5.20%	2.40%	40.13%	1.13%	49.89%	1.14%	4.81%	0.13%
40	3.70%	2.80%	48.28%	1.32%	42.76%	1.34%	5.40%	0.15%
50	9.80%	2.80%	44.52%	1.32%	40.68%	1.34%	5.04%	0.15%
60	19.10%	2.30%	40.20%	1.08%	36.23%	1.10%	4.50%	0.12%
70	27.10%	2.20%	36.01%	1.03%	32.89%	1.05%	4.01%	0.12%
80	37.90%	2.10%	28.77%	0.99%	29.96%	1.00%	3.28%	0.11%
90	51.60%	4.40%	21.33%	1.98%	24.61%	3.86%	2.45%	0.26%
100	60.70%	4.30%	15.36%	1.92%	22.09%	3.73%	1.72%	0.25%
110	69.70%	8.70%	7.93%	4.61%	21.06%	7.12%	1.21%	0.58%
120	73.30%	10.80%	8.98%	2.02%	16.55%	5.07%	1.17%	0.30%
130	78.30%	4.70%	10.56%	2.14%	10.00%	4.17%	1.13%	0.28%
140	88.80%	4.70%	5.87%	2.10%	4.74%	4.13%	0.57%	0.27%
150	92.90%	2.10%	6.40%	0.57%	0.58%	1.45%	0.12%	0.08%
160	93.50%	2.60%	6.27%	1.22%	0.00%	1.24%	0.56%	0.14%

S.I. 8 Percentage of different Fe species with time in the Cr+Fe system.

Time (min)	ferrihydrite	error	μ-oxo dimer	error	$Fe(H_2O)_6^{3+}$	error	$Fe(OH)(H_2O)_6^{2+}$	error
10	0.00%	/	29.52%	3.65%	66.41%	15.00%	4.02%	0.64%
20	0.00%	/	39.40%	4.40%	55.82%	15.38%	4.76%	0.71%
30	5.90%	9.50%	39.47%	5.05%	49.93%	7.82%	4.72%	0.63%
40	8.30%	5.40%	46.26%	0.55%	40.36%	3.62%	5.09%	0.12%
50	10.10%	2.60%	43.38%	1.22%	41.63%	1.24%	4.92%	0.14%
60	22.50%	2.50%	38.69%	1.18%	34.55%	1.19%	4.27%	0.13%
70	35.80%	3.60%	30.24%	1.63%	30.56%	3.15%	3.39%	0.21%
80	42.60%	2.20%	25.96%	1.03%	28.35%	1.05%	3.00%	0.12%
90	48.00%	9.10%	21.43%	4.83%	27.99%	7.47%	2.59%	0.60%
100	54.00%	4.30%	20.55%	1.98%	23.10%	3.86%	2.35%	0.26%
110	65.30%	4.10%	16.02%	1.87%	16.87%	3.68%	1.80%	0.24%
120	71.90%	4.80%	12.76%	0.39%	13.82%	2.46%	1.40%	0.08%
130	79.90%	2.10%	5.29%	0.57%	14.10%	1.45%	0.82%	0.08%
140	88.60%	4.80%	7.00%	2.20%	3.71%	4.31%	0.67%	0.29%
150	85.70%	3.50%	8.35%	1.65%	5.08%	1.67%	0.87%	0.19%
160	91.32%	5.70%	0.05%	0.73%	8.41%	4.81%	0.22%	0.16%

S.I. 9 R factor and ΔR factor% obtained from EXAFS LCF analysis.

	R-factor							ΔR factor%[&]				
	Time (min)	DS[*]	DS with Fh	DS with Goe	DS with Hem	DS with Aka	DS with Lep	DS with Fh	DS with Goe	DS with Hem	DS with Aka	DS with Lep
Fe system	10	0.058	0.052	0.052	0.056	0.054	0.058	-10.90%	-10.10%	-4.30%	-6.10%	-0.50%
	20	0.041	0.033	0.037	0.04	0.037	0.041	-19.51%	-8.70%	-3.50%	-8.90%	-0.40%
	30	0.042	0.033	0.039	0.041	0.038	0.042	-21.50%	-8.00%	-2.50%	-9.40%	-1.10%
	40	0.043	0.033	0.039	0.042	0.038	0.043	-25.00%	-10.70%	-4.50%	-12.20%	-2.10%
	50	0.043	0.03	0.037	0.041	0.036	0.041	-30.30%	-13.70%	-4.60%	-15.90%	-4.20%
	60	0.054	0.029	0.042	0.051	0.04	0.05	-45.40%	-22.70%	-6.20%	-26.60%	-8.00%
	70	0.062	0.028	0.044	0.056	0.04	0.057	-54.40%	-29.00%	-9.80%	-35.40%	-9.30%
	80	0.065	0.027	0.042	0.06	0.039	0.054	-58.00%	-35.20%	-7.60%	-40.50%	-17.60%
	90	0.077	0.024	0.047	0.067	0.04	0.065	-68.50%	-39.40%	-12.60%	-48.40%	-15.90%
	100	0.104	0.024	0.054	0.091	0.045	0.078	-77.30%	-47.60%	-12.40%	-56.70%	-25.20%
	110	0.12	0.024	0.059	0.104	0.047	0.088	-80.40%	-50.90%	-13.10%	-61.20%	-27.00%
	120	0.144	0.022	0.064	0.123	0.049	0.105	-84.60%	-55.40%	-14.20%	-66.00%	-27.30%
	130	0.164	0.025	0.073	0.141	0.054	0.117	-84.80%	-55.80%	-14.00%	-66.80%	-29.00%
	140	0.205	0.027	0.087	0.173	0.062	0.15	-86.80%	-57.50%	-15.60%	-69.70%	-27.00%
	150	0.226	0.026	0.092	0.191	0.065	0.16	-88.50%	-59.40%	-15.70%	-71.10%	-29.30%
	160	0.22	0.039	0.089	0.186	0.067	0.154	-82.40%	-59.60%	-15.70%	-69.70%	-30.10%
Al+Fe system	10	0.036	0.032	0.033	0.035	0.033	0.036	-11.11%	-8.80%	-3.20%	-9.90%	-0.10%
	20	0.031	0.027	0.03	0.031	0.03	0.031	-14.70%	-6.00%	-1.50%	-6.10%	0.00%
	30	0.031	0.023	0.03	0.031	0.029	0.031	-25.80%	-5.30%	-1.20%	-6.30%	-0.30%
	40	0.033	0.026	0.032	0.033	0.031	0.033	-21.21%	-10.60%	-2.50%	-6.70%	-0.30%
	50	0.036	0.028	0.032	0.035	0.031	0.036	-23.60%	-13.50%	-4.00%	-13.50%	-1.60%
	60	0.041	0.024	0.033	0.039	0.03	0.038	-41.90%	-21.50%	-4.70%	-26.10%	-6.90%

	70	0.049	0.022	0.035	0.046	0.031	0.043	-55.60%	-33.30%	-6.20%	-36.90%	-12.50%
	80	0.061	0.019	0.035	0.054	0.029	0.05	-69.50%	-43.30%	-11.40%	-53.10%	-17.90%
	90	0.092	0.021	0.048	0.08	0.038	0.072	-77.20%	-62.20%	-12.60%	-58.60%	-21.50%
	100	0.115	0.019	0.055	0.099	0.039	0.084	-83.80%	-57.90%	-13.30%	-65.70%	-26.60%
	110	0.137	0.019	0.056	0.116	0.039	0.101	-86.40%	-60.30%	-15.60%	-71.30%	-26.70%
	120	0.159	0.028	0.069	0.139	0.05	0.107	-82.20%	-64.40%	-12.10%	-68.60%	-32.20%
	130	0.192	0.021	0.072	0.16	0.046	0.135	-89.00%	-63.90%	-16.50%	-76.20%	-29.80%
	140	0.221	0.021	0.083	0.184	0.051	0.156	-90.40%	-67.20%	-16.80%	-76.90%	-29.60%
	150	0.283	0.028	0.105	0.228	0.06	0.202	-90.30%	-70.80%	-19.20%	-78.80%	-28.40%
	160	0.26	0.029	0.09	0.213	0.055	0.179	-89.00%	-59.70%	-18.10%	-78.70%	-31.20%
	10	0.033	0.028	0.031	0.032	0.03	0.033	-15.50%	-5.90%	-3.80%	-7.90%	0.00%
	20	0.026	0.024	0.025	0.026	0.025	0.026	-10.50%	-3.90%	-1.30%	-4.10%	0.00%
	30	0.029	0.023	0.027	0.028	0.027	0.029	-20.69%	-5.80%	-2.20%	-6.40%	-0.10%
	40	0.028	0.022	0.025	0.027	0.024	0.028	-22.50%	-9.70%	-4.00%	-12.50%	-0.80%
	50	0.036	0.027	0.032	0.034	0.03	0.035	-23.80%	-11.90%	-5.20%	-15.20%	-2.30%
	60	0.046	0.024	0.033	0.042	0.03	0.041	-47.40%	-27.10%	-7.00%	-33.90%	-10.30%
	70	0.059	0.019	0.036	0.051	0.029	0.052	-68.00%	-39.70%	-13.50%	-51.40%	-12.10%
Cr+Fe system	80	0.071	0.019	0.038	0.062	0.031	0.057	-73.10%	-46.90%	-12.40%	-57.10%	-19.80%
	90	0.085	0.018	0.042	0.074	0.032	0.067	-78.90%	-50.90%	-13.10%	-62.90%	-21.50%
	100	0.103	0.018	0.047	0.088	0.033	0.079	-82.30%	-54.20%	-14.30%	-68.00%	-23.70%
	110	0.13	0.017	0.051	0.107	0.034	0.097	-86.80%	-60.90%	-17.40%	-74.10%	-25.20%
	120	0.163	0.025	0.061	0.131	0.04	0.122	-84.80%	-62.60%	-19.90%	-75.20%	-25.00%
	130	0.189	0.02	0.07	0.154	0.043	0.137	-89.40%	-63.00%	-18.70%	-77.10%	-27.50%
	140	0.227	0.022	0.076	0.181	0.046	0.163	-90.10%	-66.30%	-20.20%	-79.70%	-28.00%
	150	0.24	0.021	0.087	0.203	0.059	0.16	-91.30%	-63.80%	-15.50%	-75.60%	-33.30%
	160	0.329	0.028	0.179	0.293	0.144	0.254	-91.50%	-45.60%	-10.90%	-56.20%	-22.70%

[*]DS is short for dissolved Fe species.

[&]ΔR factor%=(R-factor$_{time}$ - R-factor$_{10min}$)/R-factor$_{10min}$.

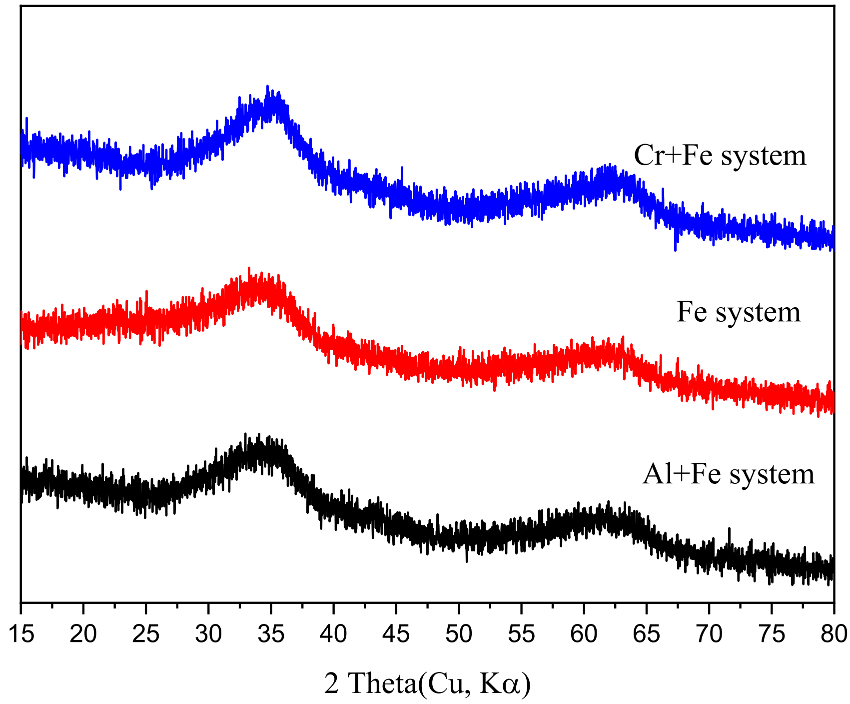

S.I. 10 XRD patterns of the solids obtained at the end of reaction in the three systems.

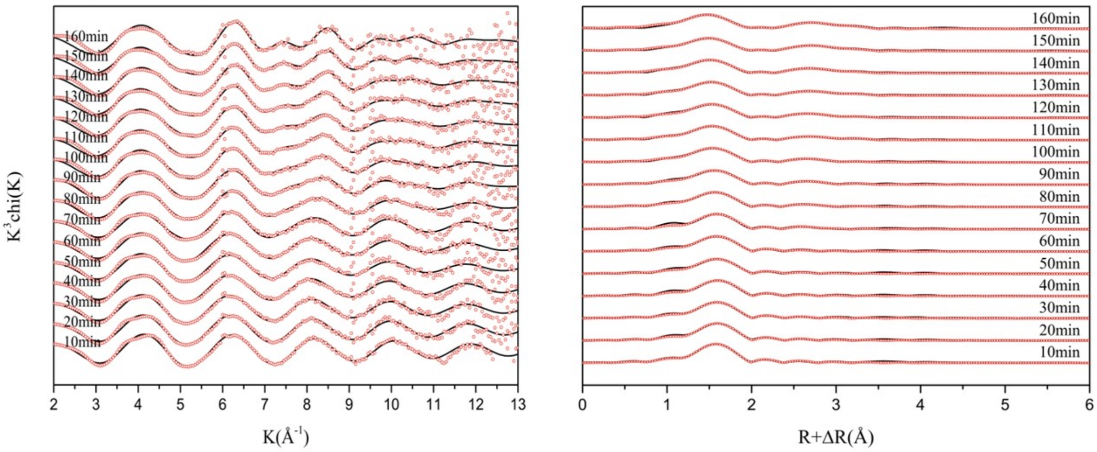

S.I. 11 Fitting results of Fe K-edge EXAFS (left) and Fourier transformed spectra of the reaction intermediates during ferrihydrite formation in Fe system (red circles is experimental data; black line is fitting data).

S.I. 12 Shell by shell fitting results of Fe K-edge EXAFS spectra of the reaction intermediates during ferrihydrite formation in the Fe system.

Time (min)	Path	CN	σ^2	E_0(eV)	R(Å)	R factor
10	Fe-O	3.8(*0.3*)	0.0040(*0.0006*)	0.29	2.012(*0.005*)	0.0122
20	Fe-O	3.5(*0.3*)	0.0040(*0.0008*)	0.83	2.026(*0.006*)	0.0182
30	Fe-O	3.6(*0.3*)	0.0048(*0.0008*)	0.34	2.028(*0.006*)	0.0163
40	Fe-O	3.4(*0.3*)	0.0046(*0.0009*)	0.99	2.034(*0.007*)	0.0222
50	Fe-O	3.7(*0.4*)	0.0060(*0.0011*)	0.07	2.030(*0.008*)	0.0269
60	Fe-O	3.7(*0.4*)	0.0056(*0.0009*)	-0.24	2.028(*0.007*)	0.0199
70	Fe-O	3.3(*0.4*)	0.0047(*0.0011*)	0.10	2.024(*0.018*)	0.0227
	$Fe-Fe_1$	0.7(*0.6*)	0.0119(*0.0126*)		3.061(*0.008*)	
80	Fe-O	4.1(*0.5*)	0.0070(*0.0011*)	-0.87	2.014(*0.015*)	0.0104
	$Fe-Fe_1$	1.3(*1.1*)	0.0132(*0.0121*)		3.060(*0.059*)	
	$Fe-Fe_2$	3.2(*1.1*)	0.0341(*0.0654*)		3.358(*0.008*)	
90	Fe-O	4.3(*0.6*)	0.0080(*0.0014*)	-0.67	2.013(*0.010*)	0.0138
	$Fe-Fe_1$	2.0(*1.7*)	0.0163(*0.0143*)		3.084(*0.049*)	
	$Fe-Fe_2$	0.6(*0.5*)	0.0078(*0.0180*)		3.383(*0.046*)	
100	Fe-O	4.6(*0.5*)	0.0083(*0.0011*)	-3.03	2.000(*0.008*)	0.0085
	$Fe-Fe_1$	2.2(*1.6*)	0.0122(*0.0071*)		3.060(*0.028*)	
	$Fe-Fe_2$	2.1(*0.7*)	0.0244(*0.0351*)		3.384(*0.067*)	
110	Fe-O	4.4(*0.4*)	0.0080(*0.0009*)	-3.32	1.996(*0.006*)	0.0058
	$Fe-Fe_1$	3.0(*2.4*)	0.0194(*0.0094*)		3.081(*0.034*)	
	$Fe-Fe_2$	1.3(*1.6*)	0.0101(*0.0079*)		3.407(*0.018*)	
120	Fe-O	4.6(*0.5*)	0.0089(*0.0011*)	-3.24	1.995(*0.008*)	0.0085
	$Fe-Fe_1$	2.9(*2.6*)	0.0157(*0.0073*)		3.067(*0.026*)	
	$Fe-Fe_2$	2.3(*1.7*)	0.0178(*0.0160*)		3.398(*0.036*)	
130	Fe-O	4.4(*0.4*)	0.0085(*0.0010*)	-3.88	1.989(*0.007*)	0.0069
	$Fe-Fe_1$	3.0(*1.8*)	0.0172(*0.0082*)		3.071(*0.033*)	
	$Fe-Fe_2$	1.7(*1.2*)	0.0119(*0.0085*)		3.408(*0.021*)	
140	Fe-O	4.8(*0.5*)	0.0095(*0.0011*)	-4.21	1.979(*0.008*)	0.0075
	$Fe-Fe_1$	2.5(*2.6*)	0.0145(*0.0082*)		3.052(*0.036*)	
	$Fe-Fe_2$	1.7(*1.8*)	0.0125(*0.0113*)		3.406(*0.034*)	
150	Fe-O	4.8(*0.4*)	0.0098(*0.0010*)	-5.68	1.975(*0.007*)	0.0055
	$Fe-Fe_1$	2.3(*1.3*)	0.0138(*0.0079*)		3.047(*0.036*)	
	$Fe-Fe_2$	1.5(*1.0*)	0.0094(*0.0082*)		3.404(*0.026*)	
160	Fe-O	5.6(*0.6*)	0.0104(*0.0010*)	-7.02	1.965(*0.007*)	0.0051
	$Fe-Fe_1$	3.5(*2.3*)	0.0156(*0.0056*)		3.056(*0.021*)	
	$Fe-Fe_2$	2.6(*1.8*)	0.0106(*0.0046*)		3.383(*0.013*)	

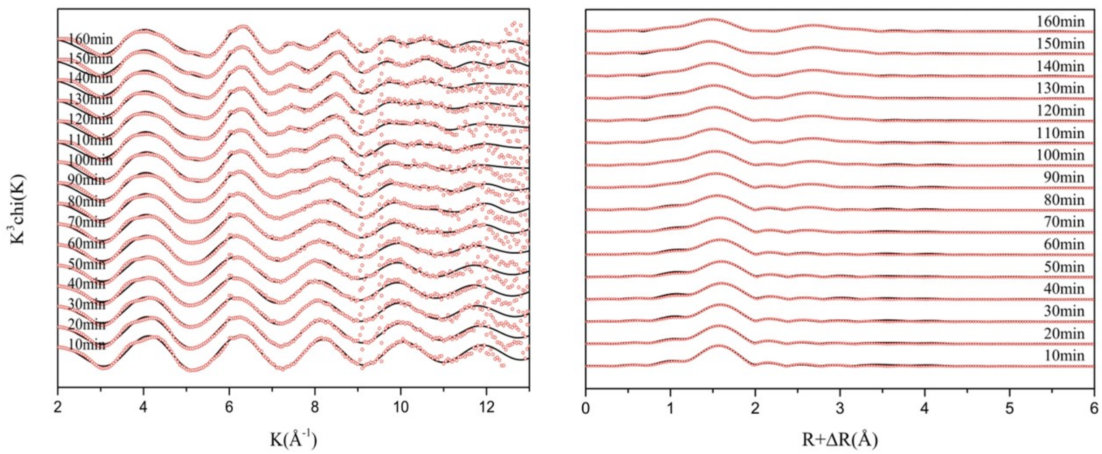

S.I. 13 Fitting results of Fe K-edge EXAFS (left) and Fourier transformed spectra of the reaction intermediates during ferrihydrite formation in Al+Fe system (red circles is experimental data; black line is fitting data).

S.I. 14 Shell by shell fitting results of Fe K-edge EXAFS spectra of the reaction intermediates during ferrihydrite formation in the Al+Fe system.

Time (min)	Path	CN	σ^2	E_0(eV)	R(Å)	R factor
10	Fe-O	4.0(*0.3*)	0.0035(*0.0006*)	-0.53	2.007(*0.005*)	0.0134
20	Fe-O	3.8(*0.3*)	0.0040(*0.0006*)	-0.97	2.014(*0.005*)	0.0117
30	Fe-O	3.6 (*0.3*)	0.0041(*0.0007*)	-0.11	2.026(*0.006*)	0.0152
40	Fe-O	3.3(*0.3*)	0.0040(*0.0009*)	0.85	2.037(*0.007*)	0.0236
50	Fe-O	3.4(*0.3*)	0.0045(*0.0008*)	0.68	2.037(*0.007*)	0.0201
60	Fe-O	3.7(*0.4*)	0.0056(*0.0009*)	-0.24	2.028(*0.007*)	0.0199
70	Fe-O	4.0(*0.4*)	0.0065(*0.0010*)	-0.84	2.022(*0.008*)	0.0155
	$Fe-Me_1$	0.2(*0.2*)	0.0003(*0.0091*)	-0.84	3.049(*0.028*)	
80	Fe-O	4.2(*0.4*)	0.0072(*0.0009*)	-2.24	2.010(*0.006*)	0.0107
	$Fe-Me_1$	0.3(*0.2*)	0.0004(*0.0047*)		3.044(*0.015*)	
90	Fe-O	4.7(*0.5*)	0.0083(*0.0011*)	-3.40	1.998(*0.008*)	0.0096
	$Fe-Me_1$	0.6(*1.1*)	0.0048(*0.0099*)		3.045(*0.030*)	
	$Fe-Me_2$	0.6(*0.7*)	0.0212(*0.0275*)		3.361(*0.087*)	
100	Fe-O	5.0(*0.5*)	0.0092(*0.0010*)	-2.98	1.994(*0.007*)	0.0070
	$Fe-Me_1$	1.1(*1.9*)	0.0133(*0.0077*)		3.047(*0.032*)	
	$Fe-Me_2$	0.9(*0.7*)	0.0094(*0.0126*)		3.392(*0.032*)	
110	Fe-O	4.7(*0.4*)	0.0084(*0.0009*)	-4.76	1.985(*0.007*)	0.0053
	$Fe-Me_1$	1.5(*1.4*)	0.0099(*0.0063*)		3.049(*0.029*)	
	$Fe-Me_2$	1.1(*1.0*)	0.0105(*0.0130*)		3.394(*0.043*)	
120	Fe-O	4.6(*0.5*)	0.0087(*0.0010*)	-4.03	1.987(*0.008*)	0.0071
	$Fe-Me_1$	2.5(*2.5*)	0.0144(*0.0081*)		3.059(*0.036*)	
	$Fe-Me_2$	1.2(*1.9*)	0.0090(*0.0098*)		3.404(*0.028*)	
130	Fe-O	4.7(*0.5*)	0.0093(*0.0011*)	-4.34	1.985(*0.008*)	0.0066
	$Fe-Me_1$	2.1(*1.9*)	0.0111(*0.0063*)		3.047(*0.030*)	
	$Fe-Me_2$	1.4(*1.6*)	0.0115(*0.0136*)		3.405(*0.045*)	
140	Fe-O	4.9(*0.5*)	0.0098(*0.0011*)	-6.15	1.971(*0.008*)	0.0062
	$Fe-Me_1$	2.2(*2.2*)	0.0119(*0.0080*)		3.038(*0.038*)	
	$Fe-Me_2$	1.3(*1.5*)	0.0080(*0.0101*)		3.398(*0.034*)	
150	Fe-O	5.1(*0.6*)	0.0104(*0.0012*)	-7.71	1.961(*0.008*)	0.0065
	$Fe-Me_1$	2.1(*2.3*)	0.0125(*0.0111*)		3.018(*0.046*)	
	$Fe-Me_2$	0.9(*1.2*)	0.0033(*0.0081*)		3.391(*0.024*)	
160	Fe-O	4.8(*0.4*)	0.0102(*0.0010*)	-5.80	1.973(*0.007*)	0.0048
	$Fe-Me_1$	1.9(*1.5*)	0.0111(*0.0078*)		3.019(*0.032*)	
	$Fe-Me_2$	0.6(*0.8*)	0.0021(*0.0086*)		3.397(*0.025*)	

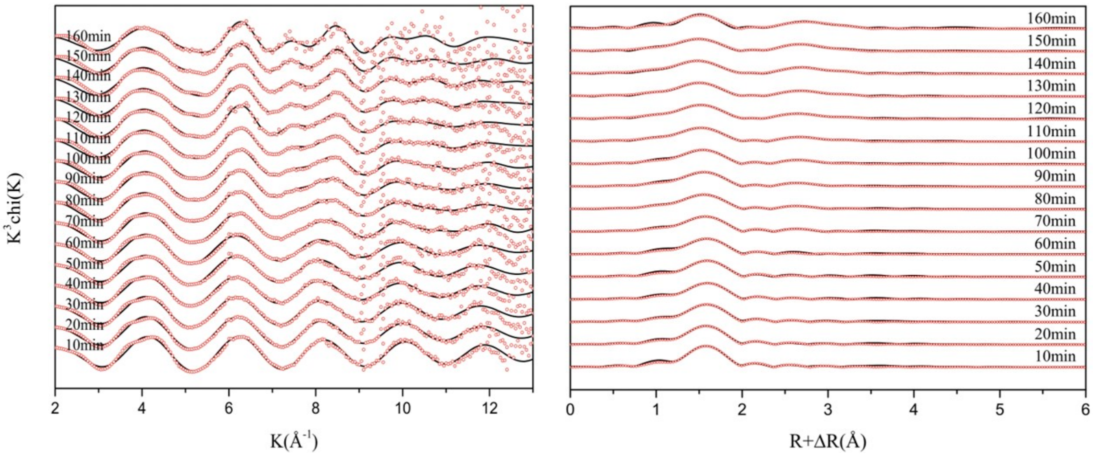

S.I. 15 Fitting results of Fe K-edge EXAFS (left) and Fourier transformed spectra of the reaction intermediates during ferrihydrite formation in Cr+Fe system (red circles is experimental data; black line is fitting data).

S.I. 16 Shell by shell fitting results of Fe K-edge EXAFS spectra of the reaction intermediates during ferrihydrite formation in the Cr+Fe system.

Time (min)	Path	CN	σ^2	E_0(eV)	R(Å)	R factor
10	Fe-O	3.8(*0.3*)	0/.0030(*0.0007*)	0.16	2.011(*0.005*)	0.0134
20	Fe-O	3.9(*0.3*)	0.0042(*0.0007*)	-0.63	2.017(*0.006*)	0.0148
30	Fe-O	3.7(*0.3*)	0.0043(*0.0007*)	-0.24	2.024(*0.006*)	0.0152
40	Fe-O	3.6(*0.3*)	0.0048(*0.0009*)	0.77	2.034(*0.007*)	0.0193
50	Fe-O	3.6(*0.4*)	0.0049(*0.0010*)	0.35	2.032(*0.007*)	0.0251
60	Fe-O	3.8(*0.4*)	0.0057(*0.0011*)	0.23	2.028(*0.008*)	0.0290
70	Fe-O	4.2(*0.4*)	0.0070(*0.0009*)	-0.59	2.017(*0.007*)	0.0108
	Fe-Me$_1$	0.3(*0.2*)	0.0013(*0.0054*)		3.042(*0.017*)	
	Fe-O	4.5(*0.5*)	0.0079(*0.0011*)		2.012(*0.008*)	
80	Fe-Me$_1$	1.5(*1.5*)	0.0117(*0.0080*)	-2.06	3.056(*0.036*)	0.0088
	Fe-Me$_2$	2.8(*2.4*)	0.0292(*0.0420*)		3.361(*0.065*)	
	Fe-O	4.5(*0.5*)	0.0080(*0.0012*)		2.009(*0.008*)	
90	Fe-Me$_1$	1.9(*1.8*)	0.0127(*0.0074*)	-1.83	3.061(*0.031*)	0.0102
	Fe-Me$_2$	3.9(*2.1*)	0.0303(*0.0353*)		3.381(*0.056*)	
	Fe-O	4.3(*0.5*)	0.0078(*0.0012*)		2.002(*0.009*)	
100	Fe-Me$_1$	2.2(*1.4*)	0.0082(*0.0075*)	-2.59	3.052(*0.024*)	0.0104
	Fe-Me$_2$	1.3(*2.4*)	0.0202(*0.0419*)		3.407(*0.111*)	
	Fe-O	4.8(*0.5*)	0.0092(*0.0010*)		1.993(*0.007*)	
110	Fe-Me$_1$	2.3(*2.0*)	0.0142(*0.0070*)	-3.95	3.059(*0.028*)	0.0066
	Fe-Me$_2$	1.5(*1.1*)	0.0121(*0.0100*)		3.391(*0.026*)	
	Fe-O	5.1(*0.4*)	0.0096(*0.0008*)	-3.95	1.991(*0.006*)	
120	Fe-Me$_1$	2.5(*2.7*)	0.0194(*0.0046*)		3.065(*0.017*)	0.0041
	Fe-Me$_2$	4.6(*3.1*)	0.0186(*0.0065*)		3.389(*0.015*)	
	Fe-O	4.9(*0.4*)	0.0095(*0.0009*)		1.980(*0.007*)	
130	Fe-Me$_1$	2.5(*2.0*)	0.0138(*0.0066*)	-5.25	3.045(*0.031*)	0.0045
	Fe-Me$_2$	1.2(*1.5*)	0.0085(*0.0076*)		3.395(*0.023*)	
	Fe-O	5.3(*0.6*)	0.0107(*0.0011*)		1.973(*0.008*)	
140	Fe-Me$_1$	2.4(*2.2*)	0.0129(*0.0078*)	-6.40	3.036(*0.036*)	0.0059
	Fe-Me$_2$	1.2(*1.5*)	0.0062(*0.0074*)		3.386(*0.023*)	
	Fe-O	4.7(*0.5*)	0.0100(*0.0011*)		1.978(*0.009*)	
150	Fe-Me$_1$	1.2(*1.0*)	0.0059(*0.0063*)	-6.02	3.021(*0.029*)	0.0064
	Fe-Me$_2$	1.0(*1.4*)	0.0066(*0.0123*)		3.419(*0.036*)	
	Fe-O	3.5(*0.7*)	0.0058(*0.0018*)		1.977(*0.014*)	
160	Fe-Me$_1$	1.8(*1.8*)	0.0092(*0.0157*)	-4.79	3.026(*0.058*)	0.0244
	Fe-Me$_2$	1.5(*1.3*)	0.0077(*0.0193*)		3.413(*0.069*)	

S.I. 17 A proposed conversion pathway of μ-oxo to dihydroxo dimer.

Step 1: dehydration (MIN1 → TS1 → MIN2): One H_2O molecule is moved from the inner-sphere to the outer-sphere.

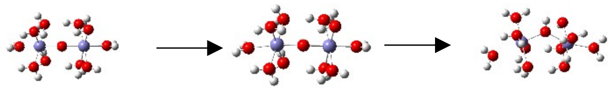

MIN1 TS1 MIN2

Step 2: protonation (MIN2 → TS2 → MIN3): The μ-oxo O gets one H^+ from a H_2O molecule. Then the H_2O molecule becomes OH.

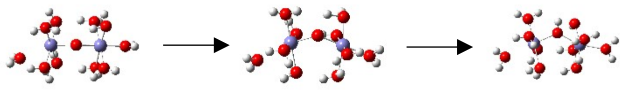

MIN2 TS2 MIN3

Step 3: ring closure (MIN3 → TS3 → MIN4): The OH-binds to the other Fe and forms a new bridge Fe–OH–Fe, and consequently, the dihydroxo bridge forms.

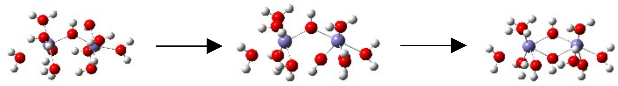

MIN3 TS3 MIN4

References

Zhu, M., Frandsen, C., Wallace, A.F., Legg, B., Khalid, S., Zhang, H., Mørup, S., Banfield, J.F., Waychunas, G.A., 2016. Precipitation pathways for ferrihydrite formation in acidic solutions. Geochimica et Cosmochimica Acta 172, 247-264.